J Food Sci Technol (January 2017) 54(1):9–17
DOI 10.1007/s13197-016-2389-3

ORIGINAL ARTICLE

Development of carboxymethyl xylan films with functional properties

Lúcia C. C. Queirós[1,2] · Sónia C. L. Sousa[1] · Andreia F. S. Duarte[2] · Fernanda C. Domingues[1,2] · Ana M. M. Ramos[1]

Revised: 13 October 2016 / Accepted: 20 October 2016 / Published online: 28 January 2017

Abstract The aim of this work was focused on the development of carboxymethyl xylan (CMX) formulations with functional properties to produce edible films. Beechwood Xylan was firstly derivatized into carboxymethyl xylan and thereafter was blended with Agar (Ag), Ammonium zirconium carbonate (AZC) and linoleic acid (La) to produce CMX:Ag, CMX:AZC, CMX:Ag:La films. Mechanical, barrier, optical and thermal properties of the produced films and their antimicrobial activity against food pathogenic bacteria were evaluated. The obtained films were transparent and yellowish. Agar and AZC improved the tensile strength at break of the control CMX film from 4.79 to 27.67 and 20.95 MPa respectively, and the CMX:AZC film exhibited the greatest elastic modulus. Barrier properties of the films decreased when any of the components was incorporated into the CMX and all blended films were thermally more stable than control. The CMX:Ag:La film revealed a good antimicrobial activity against *B. cereus* and *S. aureus*.

Keywords Carboxymethylxylan films · Mechanical properties · Barrier properties · Antimicrobial properties

✉ Fernanda C. Domingues
fdomingues@ubi.pt

[1] FibEnTech and Department of Chemistry, University of Beira Interior, Rua Marquês d'Ávila e Bolama, 6201-001 Covilhã, Portugal

[2] CICS-Health Sciences Research Centre, University of Beira Interior, Av. Infante D. Henrique, 6201-556 Covilhã, Portugal

Introduction

Waste disposals of food packaging, as well as the limited nature of fossil fuels have caused considerable concerns about its adverse effects on the environment (Azeredo et al. 2014). For this reason, there is an increasing interest by seeking new bio-based materials and eco-friendly products. In foodstuffs, one of the solutions is the use of edible films, replacing the traditional synthetic package and/or reducing its use. These edible films can act as a semipermeable barrier to water vapor, oxygen and carbon dioxide between the food and the surrounding atmosphere. They can also be used as a carrier to antimicrobial agents, which will improve simultaneously the quality and safety of food (Costa et al. 2015).

The use of biopolymer like proteins on edible/biodegradable films and their applications in the food industry has been the subject of study (Khetan and Narpinder 2015). Also polysaccharides have been widely studied. Xylans are the most abundant type of hemicelluloses and represent a promising source of renewable raw materials for the development of edible films. This polysaccharide is generally available in large quantities in wood, forest and by-products of the pulp and paper mills as well as agro industries (Gírio et al. 2010). Xylan consists of a main chain of β-(1 → 4) linked xylose units. These xylose units can have *O*-acetyl groups at position O-2 and/or O-3 and branched of carbohydrates at position C-2 and/or C-3, as the 4-*O*-methyl-D-glucuronic acid (Deutschmann and Dekker 2012).

Many efforts have been made to improve the mechanical and barrier properties of polysaccharide-based films with special emphasis on water vapour barrier. The improvement of these properties can be accomplished in several ways (Rhim and Ng 2007). For

example, the carboxymethylation of xylose yields water-soluble xylans with better ability to form films (Albertsson and Edlund 2011; Peng and She 2014; Peng et al. 2015). Additionally, ammonium zirconium carbonate (AZC) is a crosslinker that has been tested effectively on different hemicellulose based films to improve the mechanical resistance of a polysaccharide film (Mikkonen et al. 2013; Chen et al. 2015). Agar has also been regarded as a promising polymer for use in biodegradable packaging, due to the combination of its biodegradability, renewability and gelling power (Wu et al. 2009). Lipids, such as fatty acids, have commonly been used to reduce the water vapour transmission rate of hydrophilic films (Morillon et al. 2002) and according to the literature, some fatty acids, besides improving the barrier to water vapour, have the ability to inhibit the growth of bacteria (Desbois and Smith 2010).

In this work films of carboxymethyl xylan crosslinked with Ag, AZC and linoleic acid were produced. Mechanical, barrier, thermal, optical and antimicrobial properties of these films were evaluated in order to know its suitability for edible films.

Materials and methods

Materials

Xylan (MW = 9.5 kDa), agar and glycerol were acquired from Sigma, SAFC and Merck, respectively. AZC 27.705 % and sodium monochloroacetate (SMCA) were obtained from Sigma-aldrich and linoleic acid from Tokyo Chemical Industry (TCI).

Preparation of CMX

Derivatization of native xylan was performed following the method described by Petzold et al. (2006). Xylan (10 g) was dissolved in 50 mL of 25 % aqueous NaOH (w v^{-1}) and the dissolution was carried out at 30 °C. After the dissolution, 70 mL of 2-propanol were added to the slurry medium and the reaction mixture was vigorously stirred at the same temperature for 30 min. Subsequently, 8.78 g of SMCA were added, and the temperature was increased to 65 °C. The reaction with SMCA was held for 70 min and then neutralized with acetic acid (2 M). The CMX was precipitated with ethanol and washed once with 100 mL of 65 % aqueous ethanol (v v^{-1}) and four times with 100 mL of ethanol (100 %). The product was dried at room temperature and the degree of substitution (DS) was determined by ^{1}H NMR analysis according to Sousa et al. (2016).

Characterization of CMX

The chemical structure of CMX was characterized by NMR. CMX was dissolved in deuterated water (10 mg mL^{-1}) and the ^{1}H spectrum was obtained at 25 °C on a Bruker Avance III 400 MHz spectrometer operating at 400.13 MHz with a Bruker standard pulse program (zg). The number of scans was 32. Sodium 3-(trimethylsilyl)propionate-*d4* (TMSP, δ 0.00) was used as internal standard.

Preparation of films

The films based on CMX were prepared by the casting method. CMX was dissolved in deionized water (0.5 % w w^{-1}) at room temperature. Glycerol (0.25 % w w^{-1} for control and CMX:Ag, 0.3 % w w^{-1} for CMX:AZC and 0.2 % w w^{-1} for CMX:Ag:La) was added as plasticizer and the mixture was kept under magnetic stirring for 5 min. Subsequently, for the CMX:Ag and CMX:AZC films a crosslinking agent, 0.25 % agar or AZC (w w^{-1}) was added and the mixture was heated at 70 or 60 °C respectively and stirred for 30 min. As to the CMX:Ag:La formulation, 0.7 % linoleic acid (w w^{-1}) was added blended with the agar. All films underwent two stages of homogenization (Ultra-Turrax T25 homogenizer IKA brand), the first at 7600 rpm for 2 min, and the second at 12,000 rpm for 2 min. The mixture was cast into a glass Petri dish, and dried at 30 °C.

Grammage, thickness and mechanical properties

The grammage of the films was obtained by the ratio between the mass and the area of the film (g m^{-2}). Films were weighed in an analytical balance (±0.0001 g). The thickness of the films was measured on a micrometer (Adamel Lhomargy model MI 20) and the average of six random measurements on the film was considered.

The mechanical properties of the films were measured with a tensile testing machine (Thwing-Albert Instrument Co.), at 22 °C and 50 % of relative humidity (RH) based on ISO 1924/1 standard with some changes to the conventional method. The films were cut into samples of 80 mm length and 15 mm width. The assay was performed at 10 mm min^{-1} and an initial grip distance of 50 mm. Four replicates were made for each film sample. Data from tensile strength at break (TS), tensile index (TI) and elastic modulus (EM) are displayed in Table 1.

Barrier properties

The surface wettability of the films was evaluated by the contact angle with water. The measurement of contact

Table 1 Grammage, thickness, mechanical and barrier properties of the films

Properties	Films			
	Control	CMX:Ag	CMX:AZC	CMX:Ag:La
Grammage (g m^{-2})	74.81 ± 12.54	89.35 ± 3.93	74.25 ± 9.43	89.25 ± 2.08
Thickness (μm)	51.27 ± 15.38	56.42 ± 1.06	47.00 ± 2.02	73.67 ± 0.19
Mechanical				
TI (N m g^{-1})	3.25 ± 0.44	17.48 ± 0.73	12.27 ± 1.57	14.30 ± 0.89
TS (MPa)	4.79 ± 1.10	27.67 ± 0.97	20.95 ± 3.02	17.35 ± 0.83
EM (MPa)	188.43 ± 45.96	1043.12 ± 36.98	1164.64 ± 96.15	616.26 ± 29.89
Barrier				
Contact angle (°)	37.32 ± 1.65	50.66 ± 1.10	52.45 ± 3.79	69.69 ± 2.48
WVTR (g d^{-1} m^{-2})	109.82 ± 5.40	68.76 ± 7.43	90.48 ± 6.42	46.79 ± 0.68
WVP × 10^{-6} (g d^{-1} m^{-1} Pa^{-1})	3.39 ± 0.18	3.07 ± 0.51	2.93 ± 0.35	2.63 ± 0.01
OTR (cm^3 m^{-2} d^{-1})	30.50 ± 0.71	3.00 ± 1.41	12.00 ± 2.83	[a]
OP (cm^3 μm m^{-2} d^{-1} kPa^{-1})	15.83 ± 1.30	1.96 ± 1.03	5.86 ± 2.23	–

Values are given as mean ± standard deviation

[a] The obtained values were below the lower limit of the range measuring device (0.01 $cm^3m^{-2}d^{-1}$)

angle was performed at OCHA 200 DataPhysics instrument using the sessile drop method, at 22 °C and 50 % RH. Six measurements were done at different positions of the film surface, and the average value was calculated.

Water vapor permeability (WVP) of the films was measured by the gravimetric method according to ASTM E96-1995, using the Regmed—PVA/4 equipment model. Each film was placed on an aluminum box into which has previously been placed granulated anhydrous calcium chloride as desiccant (0 % RH). Then, the films were sealed with melted paraffin and the test sample assemblies were placed into a climate room at 22 °C and 50 % HR. The exposed film area was 50 cm^2. Finally, the test sample assemblies were weighed every 2 h for 48 h. The measurements were performed in triplicate and the values were used to plot the graph of mass change (m) over time (t). The water vapor transmission rate (WVTR) was calculated by the ratio between the straight slope ($\Delta m/\Delta t$) and the area in m^2. After WVP was calculated by the following equation:

$$WVP = \frac{WVTR}{\Delta P} = \frac{WVTR}{P(R_1 - R_2)} \times e \quad (1)$$

where ΔP is the difference in vapor pressure between both sides of the film; e is the average film thickness (m) and P is the vapor saturation pressure of water at 22 °C. R_1 is the RH of the laboratory and R_2 is the RH inside the aluminum box.

The oxygen transmission rate (OTR) was measured according to ASTM F1927-14 using an OX-TRAN2/21 MOCON Tester equipped with a coulometric oxygen sensor. The samples with an exposed area of 5 cm^2 were clamped into the diffusion cell. Pure oxygen was introduced into the outside chamber of the diffusion cell. The permeation rate through the sample was measured until steady state was reached. Oxygen permeability (OP) was achieved by normalizing the OTR with respect to the oxygen pressure and the samples thickness, using the Eq. 2. The measurements were done at 23 ± 0.5 °C and 50 ± 3 % RH and performed on three replicates of each sample.

$$OP = \frac{OTR}{\Delta PO_2} \times e \quad (2)$$

where e is the average thickness of the film (μm), ΔPO_2 is the difference of oxygen partial pressure (in Pa) between the two sides of the film.

Optical properties and morphology of the films

Color and transparency of the films were evaluated using a Technidyne Color Touch 2 Model ISO Spectrophotometer. Measurements were performed on three random positions of the films using the D65 illuminant and 10° observer. CIE L*a*b* color coordinates were determined, lightness (L*), redness (a*, ±red–green) and yellowness (b*, ±yellow–blue). Transparency was calculated according to Popson et al. (1996).

The morphology of the films was observed using a Hitachi S-3400N scanning electron microscope. Before performing Scanning electron microscopy (SEM) analysis, the films were kept in a desiccator for approximately three weeks. To access the cross section, the films were fractured with a thin blade. Subsequently, film samples were placed

on aluminum brackets and sprayed with gold using a metal evaporator (Quorum Q150R ES). All images were recorded at an accelerating voltage of 20 kV.

Thermal analysis of the films

Thermogravimetric analysis (TGA) was performed using a Q50 TGA (TA Instruments). Approximately 3 g of the film was placed in a platinum pan and heated from 0 to 500 °C with a heating rate of 5 °C min^{-1} under a nitrogen flow of 40 mL min^{-1}.

Antimicrobial activity of the films

The antimicrobial activity of the films was tested against 4 bacteria strains, 2 Gram-positive strains (*B. cereus* ATCC 11778, *S. aureus* ATCC 25923) and 2 Gram-negative (*Escherichia coli* ATCC 25922 and *Salmonella typhimurium* ATCC 13311), using the agar diffusion method, according to M2–A8 standard of The National Committee for Clinical Laboratory Standards, with some modifications. Film discs with 10 mm diameter were aseptically cut from each film. The bacterial inoculums were prepared in a sterile solution of 0.85 (w v^{-1}) sodium chloride and adjusted to an optical density of 0.5 McFarland units [$\approx 1 \times 10^8$ colony forming U/mL (CFU mL^{-1})]. Then Mÿeller-Hinton Agar plates were inoculated with the inoculum, allowed to dry and the film discs were placed over the agar. The plates were incubated at 37 °C for 24 h and subsequently, the diameter (mm) of the inhibition zone surrounding film disks was measured. Finally, the contact area of the films with the agar surface was visually examined. Assays were performed in triplicate for each film in different days.

Results and discussion

Characterization of CMX by RMN

The ^{1}H NMR of CMX, shown in Fig. 1, presents three important groups of protons. The protons of non-substituted D-xylose units of the backbone, characterized by the signs: $\delta_{H2} = 3.30$, $\delta_{H5ax} = 3.38$, $\delta_{H3} = 3.56$, $\delta_{H4} = 3.79$, $\delta_{H5eq} = 4.10$ and $\delta_{H1} = 4.50$ ppm. The proton of 4-*O*-methylglucuronic acid characterized by the sign $\delta_{H1} = 5.30$ ppm (Belmokaddem et al. 2011). The anomeric protons of D-xylose monomers, on which the introduction of carboxymethyl group occured at the O-2 and O-3 positions with the chemical shifts: $\delta = 4.54$ and 4.58 ppm. The signal at 4.63 ppm corresponded to D-xylose units containing methylglucuronic groups at O-2 position. The ^{1}H NMR was also used to determine the DS of CMX. The integration ratio of these last three signals and integration of the signals for the anomeric proton of D-xylose unsubstituted and substituted with MeGlcA determines the DS of CMX. The DS obtained was 0.3.

Mechanical properties

The mechanical properties of the control, CMX:Ag, CMX:AZC and CMX:Ag:La films are shown in Table 1. The incorporation of the various components with CMX improved the mechanical properties of films as compared

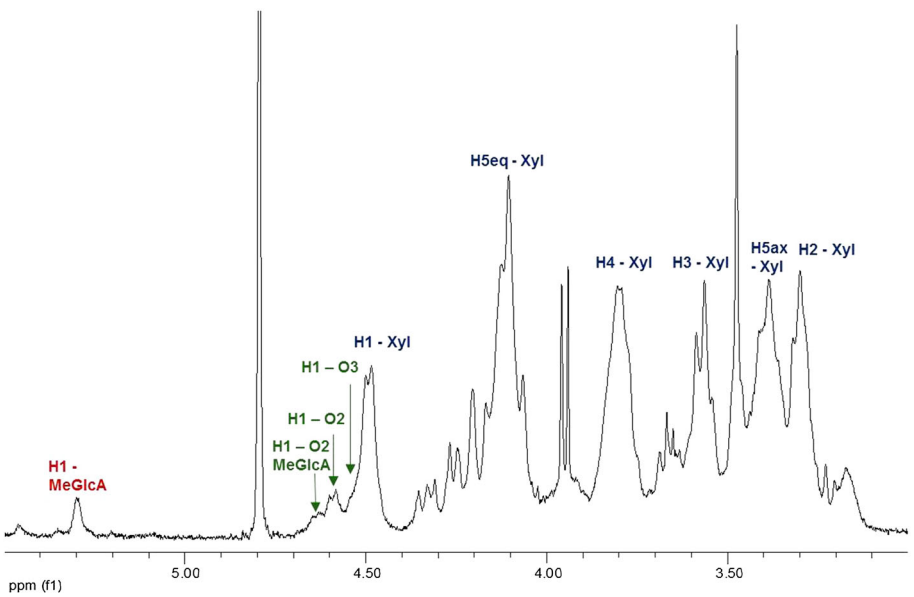

Fig. 1 ^{1}H NMR spectrum of CMX. Xyl Hx corresponds to the protons present in the D-xylose units and MeGlcA to Hx protons of 4-*O*-methylglucuronic acid and ax and eq correspond to conformations of protons, axial and equatorial respectively

to the control. Similar results were reported by other authors (Shevkani and Singh 2015; Yu-Yue et al. 2015; Jafarzadeh et al. 2016) respectively with proteins, chitosan and semolina. The increase in mechanical properties can be explained by the formation of hydrogen bonds. The formation of these new links increased the cohesion between the polymer chains of CMX, preventing its separation and increasing the maximum force required to break the film (Guilbert et al. 1996). The improvement of mechanical properties generated by the crosslinking agents, in particular AZC and agar, have been previously observed for poly (vinyl alcohol):xylan films (Chen et al. 2015) and starch film incorporated with agar (Wu et al. 2009).

Comparing CMX:Ag and CMX:AZC films, it can be observed that the first has higher TS and TI than the second. This result may be due to the greater amount of plasticizer in the film with AZC. Even though the film crosslinked with AZC has lower TS than the film CMX:Ag, it showed the highest EM. The EM determined the rigidity of a film, the higher the EM of the film, the lowered the elastic deformation and the greater its rigidity (Callister 2001). The results revealed that the AZC had a better ability to interact with the polymer chains of CMX than agar.

Concerning CMX:Ag:La and CMX:Ag films, the results showed that the incorporation of linoleic acid decreased drastically the mechanical properties of the film. This trend has been reported by Pérez-Gago and Rhim (2014). The negative effect of linoleic acid on the mechanical properties can be due to the presence of a large amount of hollows throughout the film thickness, as verified through the SEM analysis (data not shown). These hollows prevented the interaction between the polymer chains decreasing the mechanical properties of the film.

Barrier properties

Barrier properties, namely wettability, WVP and OTR are shown in Table 1. Concerning wettability given by the contact angle it was observed that the control film has the lowest value. Thus, it can be noted that this film has a hydrophilic surface. Its hydrophilic nature was given by the presence of carboxymethyl and hydroxyl groups in the CMX (Alekhina et al. 2014). The value obtained was comparable to the CMX film without plasticizer produced by Velkova et al. (2015). Regarding the other films, the contact angle increased when the CMX is incorporated with agar, AZC or linoleic acid in this order. Despite the presence of these compounds increased the contact angle of the films, according to Karbowiak et al. (2006) only the film with lipids have a hydrophobic surface. The CMX:Ag and CMX:AZC have similar contact angle. The hydrophobicity of these two films could be explained by the decrease of hydrophilic groups (OH) available in CMX after the crosslinking reaction between compounds.

According to the data shown in Table 1 linoleic acid, AZC and agar have a similar influence on the WVP of the CMX film when compared to the control film. These results were in agreement with those obtained for the wettability. The incorporation of agar or AZC as well as linoleic acid on the formulation reduced the WVP of the films, possibly due to the formation of compact and tortuous structures, which prevented the migration of water molecules through the film (Wu et al. 2002). Also the higher hydrophobicity, due to the decrease of hydrophilic groups may attributed to this (Azeredo et al. 2014). Similar effect, even though with higher WVP were achieved by Yu-Yue et al. (2015) and Jafarzadeh et al. (2016) with chitosan and semolina films mixed with nanoclays.

The CMX:Ag:La had the lowest WVP when compared to control, CMX:Ag and CMX:AZC films. This result was expected, since the incorporation of linoleic acid reduced the ratio between the hydrophilic and hydrophobic character of the films, which lowered its solubility in water and hence its permeability to water vapor (Azeredo et al. 2014). According to Wu et al. (2002) lipids increase the complexity of the film matrix, resulting in an increase in porosity and also the distance that water molecules have to cross in the film. A large number of voids into the film may make the path of the water molecules difficult through the film. The improved WVP with addition of fatty acids to a matrix of xylan was reported earlier (Péroval et al. 2002). Comparing the WVP of CMX:Ag and CMX:AZC films, the latter was slightly better than the former. These results suggested that the AZC had better crosslinking ability than the agar.

Regarding OTR and OP data, the CMX:Ag film has better OP than the CMX:AZC film rather than that observed to WVP. Probably these results may be due to the higher thickness of the CMX:Ag film. According to Park and Chinnan (1995) the increase of film thickness leads the decrease in OP and the increase in WVP. The incorporation of AZC or agar into CMX made the films more compact due to the hydrogen bonds created between the polymers (Martín-Belloso et al. 2009) and therefore, the free volume between polymer chains is reduced lowering the OP (Müller et al. 2012). The higher rigidity of the film reduced the mobility between the polymer chains, and consequently hindered the passage of oxygen molecules. CMX:Ag:La film was not measured the OP since the value was below the detectable limit of the device. The incorporation of hydrophobic substances to CMX and agar films decreased the OP. Also the control film had a good OP performance when compared to similar films documented in the literature (Escalante et al. 2012; Alekhina et al. 2014).

Table 2 Transparency and L*a*b* color coordinates of the films

Film	Transparency	L*	a*	b*
Control	93.25 ± 0.39	88.76 ± 0.63	0.52 ± 0.20	23.19 ± 2.27
CMX:Ag	94.14 ± 1.11	88.29 ± 0.11	0.45 ± 0.02	22.45 ± 0.05
CMX:AZC	95.38 ± 0.92	90.30 ± 0.62	−0.18 ± 0.06	16.51 ± 2.15
CMX:Ag:La	90.59 ± 0.34	89.82 ± 0.20	1.05 ± 0.03	17.23 ± 0.25

Optical properties and morphology of the films

In general, the films exhibit high transparency as shown by the data on Table 2. However, the presence of linoleic acid led to a slight decrease in transparency. This outcome can be associated with the behavior of light striking a surface with lipids. It was also observed in the SEM analysis that the CMX:Ag:La film, as well as the control, exhibit a less uniform cross-section as compared to the other films. The CMX:AZC and CMX:Ag films exhibited similar transparency and both are more transparent than the control. This outcome is certainly consequence of an even surface and a more regular cross section.

All films have high values of L*, which means that they have a clear appearance and exhibit a yellow color as evidenced by the high values of b*. The control and CMX:Ag films are considerably more yellow than the CMX:Ag:La and CMX:AZC films. It should be noted that the addition of different materials to the control film reduces its yellowish. Polysaccharides-based films have higher transparency against protein-based films (Shevkani and Singh 2015). However it should be noted the lower thickness of the first films, presented in this work, which influences this property.

The structure of the control film is heterogeneous due to their irregular cross-section (Phan The et al. 2009). These film appeared to be less compact than the other films. The cross section of the CMX:Ag film exhibited a structure with two layers. The top layer was more compact than the bottom being this layer similar to the control film. According to the those authors this layer corresponded to the agar. Morris (2006) suggests that when two polymers associated independently to form separate networks which interlace, the formed structure was called an interpenetrating network. The agar is a polysaccharide with ability to form gel, so it can be assumed that a network is formed between CMX and agar when the temperature of the film formulation decreased. However, during the drying of the film, the agar network retracted, lowering the interstitial space available to retain CMX, thus lead to a phase separation in the film structure. Possibly intermolecular interactions may also occured by hydrogen bonds between agar and CMX, since both had available hydroxyl groups.

With respect to the CMX:AZC film, this presented a structure with three layers: two similar outer layers and an inner layer different from the others. Although it was possible to observe layers in the CMX:AZC film, they appeared to be linked, i.e., separation was not as obvious as in the CMX:Ag film. During the drying process, a structural organization between CMX and AZC may occured. Probably, the outer layers corresponded to the CMX crosslinked with AZC, due to its more compact appearance and the inner layer corresponded to the CMX.

The film containing linoleic acid (CMX:Ag:La) was different from the others. The cross-section revealed a heterogeneous structure in which lipid particles were retained discontinuously in the polymer matrix forming a large amount of hollows which give rise to a rough surface.

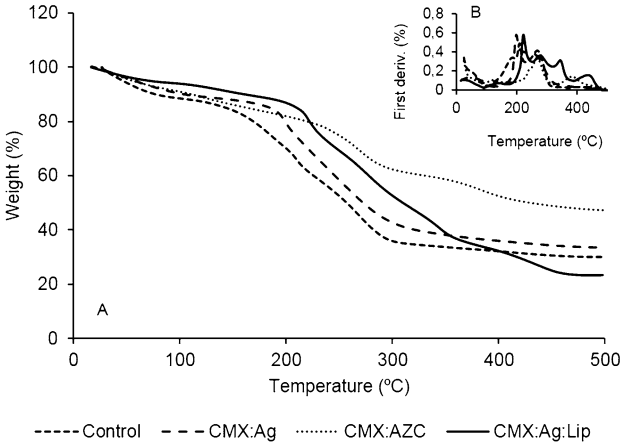

Fig. 2 Thermogravimetric curves of the films, A–TG and B-first deriv. TG

Thermal properties of the films

Thermal properties of the films are presented in Fig. 2. All the films exhibited various stages of thermal degradation. The first step of weight loss was common to all films, occurring around 100 °C and was associated to water loss, which can be chemically and physically bounded to the film constituents (Reddy and Rhim 2014). In this step, the larger amount of water loss can be observed in the control film, approximately 12 % and the smallest loss in the CMX:Ag:La film, about 5 %. These results showed the hydrophilic character of the control film and the hydrophobic character of the film with linoleic acid. The

second stage, also common to all films with the exception of the CMX:AZC, begun at approximately 180 °C, and ended at 252 °C by revealing small difference in between films. This may be usually attributed to the volatilization of glycerol.

Subsequent steps can be differentiated between the films. In the case of control film, the last step of mass loss was attributed to the degradation of CMX. This occurred between 228 and 313 °C, registering a mass loss of 22 % for this temperature range. These results were consistent with earlier study (Alekhina et al. 2014). In the CMX:Ag film, the third thermal degradation step was located between 214 and 339 °C, which probably corresponded to the thermal degradation of both polymers, CMX and agar. In this step there was a weight loss of 34 %. For the CMX:AZC film, a less pronounced mass loss can be observed when compared to the other films. The second thermal degradation step occured between 93 and 149 °C with a weight loss of 5 %, which may resulted from the liberation of water molecules coordinated with the zirconium (Sako and Sakai 2013). Then, between 194 and 312 °C a mass loss of about 21 % was recorded, which was associated with the decomposition of xylan and glycerol. Subsequently, at temperatures between 331 and 433 °C, the last step occured with approximately 10 % of mass loss, which may be related to the crystallization of AZC (Sako and Sakai 2013). Concerning the CMX:Ag:La film, between 183 and 483 °C three successive mass losses occured. The first peak at 222 °C corresponds to the volatilization of glycerol. The second peak at 279 °C may be associated with thermal degradation of CMX and agar. The third peak at 344 °C, corresponded to the evaporation of linoleic acid and/or derivatives of their degradation products (Kapusniak and Siemion 2007).

After the thermal degradation, percentages of residual mass at 500 °C were 30, 34, 47 and 23 %, respectively for the control, CMX:Ag, CMX:AZC and CMX:Ag:La films. The residual mass of CMX complies with other study (Alekhina et al. 2014). The high residual mass in the control and CMX:Ag films may be associated to the quantity of salts, which may come from the derivatization process of native xylan or the extraction and purification processes of the native xylan (Ren and Sun 2010). In fact, we verified that the salts content of CMX determined as ash content is high (20.8 %) against 6.7 % of native xylan. The residual mass on the film with linoleic acid is probably related to the formation of inorganic compounds. The CMX:AZC film has the higher residual mass, probably due to incomplete degradation and the formation of by-products resulting from the AZC decomposition (Rubio et al. 2009). The results suggest that the incorporation of different materials in CMX films improves their thermal stability.

Antimicrobial activity of the films

The antimicrobial potential against several foodborne pathogen of developed films was evaluated to see their potential utilization for food packaging (Table 3). CMX:Ag:La film was the only one that exhibited antimicrobial activity. Some fatty acids, such as linoleic acid, have the ability to inhibit the growth of bacteria (Desbois and Smith 2010).

The control film showed no antimicrobial activity against the microorganisms under study, since most xylans and its derivatives had no antimicrobial activity (Ebringerová 2012). It should be noted that the control film was dissolved in the culture medium; this behavior was due to their higher hydrophilic nature in comparison to other films. Regarding the films with cross-linking agents (CMX:Ag and CMX:AZC) no antimicrobial activity was observed. In contrast, CMX:Ag:La film, was the only one showed antimicrobial activity against Gram-positive bacteria, *B. cereus* and *S. aureus*. In general, the lower susceptibility of Gram-negative organisms to the action of antimicrobial agents may be explained by the presence of an outer membrane surrounding the cell wall of these organisms, limiting the diffusion of hydrophobic compounds through their lipopolysaccharide coating (Burt 2004). The antibacterial activity of fatty acids was influenced by its structure and shape and depended on the length of the aliphatic chain and the number of double bonds. Unsaturated long chain fatty acids tended to be more active against Gram-positive than Gram-negative

Table 3 Antimicrobial activity of CMX based films

Film	Inhibition zone diameter (mm)			
	B. cereus	*S. aureus*	*E. coli*	*S. typhimurium*
Control	0.00[a] ± 0.00	0.00[a] ± 0.00	0.00[a] ± 0.00	0.00[a] ± 0.00
CMX:Ag	10 ± 0.00	10 ± 0.00	10 ± 0.00	10 ± 0.00
CMX:AZC	10 ± 0.00	10 ± 0.00	10 ± 0.00	10 ± 0.00
CMX:Ag:La	16 ± 0.71	20 ± 0.71	10 ± 0.00	10 ± 0.00

[a] It was dissolved in the culture medium

bacteria. However, the exact mechanism by which fatty acids exert their activity against bacteria has not been documented in the literature. Among the Gram-positive bacteria, *S. aureus* was the most susceptible bacteria to the action of linoleic acid, which may be associated to differences in cell wall structure, shape and spores form ability of *B. cereus* (Muppalla et al. 2014).

Conclusion

Properties of CMX films were significantly improved with crosslinking agents and linoleic acid. The obtained films exhibited higher tensile strength at break, elastic modulus and hydrophobicity, and showed less yellowness as compared to the control films. The incorporation of crosslinking agents and linoleic acid also increased the thermal stability of CMX film. The inclusion of linoleic acid into CMX film provided a lower WVP, OP and also lower antimicrobial activity against the Gram-positive bacteria. These results suggested that the properties of CMX films were improved by crosslinking agents and linoleic acid, making them a promising application for food packaging.

References

Albertson AC, Edlund U (2011) Synthesis, chemistry and properties of hemicelluloses. In: Plackett D (ed) Biopolymers: new materials for sustainable films and coatings, 1st edn. Wiley, West Sussex, pp 133–150

Alekhina M, Mikkonen KS, Alén R et al (2014) Carboxymethylation of alkali extracted xylan for preparation of bio-based packaging films. Carbohydr Polym 100:89–96

Azeredo HMC, Rosa MF, Souza Filho MSM, Waldron KW (2014) The use of biomass for packaging films and coatings. In: Waldron K (ed) Advances in biorefineries: biomass and waste supply chain exploitation, 1st edn. Woodhead Publishing, Cambridge, pp 819–874

Belmokaddem FZ, Pinel C, Huber P et al (2011) Green synthesis of xylan hemicellulose esters. Carbohydr Res 346:2896–2904

Burt S (2004) Essential oils: their antibacterial properties and potential applications in foods—a review. Int J Food Microbiol 94:223–253

Callister WD (2001) Fundamentals of materials science and engineering: an interactive, 5th edn. Wiley, New York

Chen X, Ren J, Meng L (2015) Influence of ammonium zirconium carbonate on properties of poly (vinyl alcohol)/xylan composite films. J Nanomater. doi:10.1155/2015/810464

Costa MJ, Cerqueira MA, Ruiz HA et al (2015) Use of wheat bran arabinoxylans in chitosan-based films: effect on physicochemical properties. Ind Crops Prod 66:305–311

Desbois AP, Smith VJ (2010) Antibacterial free fatty acids: activities, mechanisms of action and biotechnological potential. Appl Microbiol Biotechnol 85:1629–1642

Deutschmann R, Dekker RFH (2012) From plant biomass to bio-based chemicals: latest developments in xylan research. Biotechnol Adv 30:1627–1640

Ebringerová A (2012) The potential of xylans as biomaterial resources. In: Habibi Y, Lucia LA (eds) Polysaccharide buildings blocks: sustainable approach to the development of renewable biomaterials, 1st edn. Wiley, New Jersey, pp 331–365

Escalante A, Gonçalvesa A, Bodina A et al (2012) Flexible oxygen barrier films from spruce xylan. Carbohydr Polym 87:2381–2387

Gírio FM, Fonseca C, Carvalheiro F et al (2010) Hemicelluloses for fuel ethanol: a review. Bioresour Technol 101:4775–4800

Guilbert S, Gontard N, Gorris LGM (1996) Prolongation of the shelf-life of perishable food products using biodegradable films and coatings. LWT Food Sci Technol 29(1–2):10–17

Jafarzadeh S, Alias AK, Ariffin F, Mahmud S, Najafi A (2016) Preparation and characterization of bionanocomposite films reinforced with nano kaolin. J Food Sci Technol 53(2):1111–1119

Kapusniak J, Siemion P (2007) Thermal reactions of starch with long-chain unsaturated fatty acids. Part 2. Linoleic acid. J Food Eng 78:323–332

Karbowiak T, Debeaufort F, Champion D, Voilley A (2006) Wetting properties at the surface of iota-carrageenan-based edible films. J Colloid Interface Sci 294:400–410

Martín-Belloso O, Rojas-Graü MA, Soliva-Fortuny R (2009) Delivery of flavor and active ingredients using edible films and coatings. In: Embuscado ME, Huber KC (eds) Edible films and coatings for food applications, 1st edn. Springer, New York, pp 295–313

Mikkonen KS, Schmidt J, Vesterinen A-H, Tenkanen M (2013) Crosslinking with ammonium zirconium carbonate improves the formation and properties of spruce galactoglucomannan films. J Mater Sci 48:4205–4213

Morillon V, Debeaufort F, Blond G et al (2002) Factors affecting the moisture permeability of lipid-based edible films: a review. Crit Rev Food Sci Nutr 42:67–89

Morris VJ (2006) Bacterial polysaccharides. In: Stephen AM, Phillips GO, Williams PA (eds) Food polysaccharides and their applications, 2nd edn. CRC Press, Boca Raton, pp 413–454

Müller CMO, Yamashita F, Grossmann MVE, Mali S (2012) Films and coatings produced from biopolymers and composites. In: Telis VRN (ed) Biopolymer engineering in food processing, 1st edn. CRC Press, Boca Raton, pp 145–216

Muppalla SR, Kanatt SR, Chawla SP, Sharma A (2014) Carboxymethyl cellulose–polyvinyl alcohol films with clove oil for active packaging of ground chicken meat. Food Packag Shelf Life 2:51–58

Park HJ, Chinnan MS (1995) Gas and water vapor barrier properties of edible films from protein and cellulosic materials. J Food Eng 25:497–507

Peng P, She D (2014) Isolation, structural characterization, and potential applications of hemicelluloses from bamboo: a review. Carbohydr Polym 112:701–720

Peng P, Zhai M, She D, Gao Y (2015) Synthesis and characterization of carboxymethyl xylan-g-poly(propylene oxide) and its application in films. Carbohydr Polym 133:117–125

Pérez-Gago MB, Rhim J-W (2014) Edible coating and film materials: lipid bilayers and lipid emulsions. In: Han JH (ed) Innovations in Food Packaging, 2nd edn. Academic Press, London, pp 325–345

Péroval C, Debeaufort F, Despré D, Voilley A (2002) Edible arabinoxylan-based films. 1. Effects of lipid type on water vapor permeability, film structure, and other physical characteristics. J Agric Food Chem 50:3977–3983

Petzold K, Schwikal K, Heinze T (2006) Carboxymethyl xylan—synthesis and detailed structure characterization. Carbohydr Polym 64:292–298

Phan The D, Debeaufort F, Voilley A, Luu D (2009) Biopolymer interactions affect the functional properties of edible films based on agar, cassava starch and arabinoxylan blends. J Food Eng 90:548–558

Popson SJ, Malthouse DD, Crawford TB et al (1996) Measurement and control of the optical properties of paper, 2nd edn. Technidyne Corporation, New Albany

Reddy JP, Rhim J-W (2014) Characterization of bionanocomposite films prepared with agar and paper-mulberry pulp nanocellulose. Carbohydr Polym 110:480–488

Ren J-L, Sun R-C (2010) Hemicelluloses. In: Sun R-C (ed) Cereal straw as a resource for sustainable biomaterials and biofuels, 1st edn. Elsevier, Amsterdam, pp 73–130

Rhim J-W, Ng PKW (2007) Natural biopolymer-based nanocomposite films for packaging applications. Crit Rev Food Sci Nutr 47:411–433

Rubio E, Rodriguez-lugo V, Rodriguez R, Castaño VM (2009) Nano zirconia and sulfated zirconia from ammonia zirconium carbonate. Rev Adv Mater Sci 22:67–73

Sako R, Sakai J (2013) Effect of curing temperature on coating structure and corrosion resistance of ammonium zirconium carbonate on galvanized steel surface. Surf Coat Technol 219:42–49

Shevkani K, Singh N (2015) Relationship between protein characteristics and film-forming properties of kidney bean, field pea and amaranth protein isolates. Int J Food Sci Technol 50:1033–1043

Sousa S, Pedrosa J, Ramos A, Ferreira PJ, Gamelas JAF (2016) Surface properties of xylan and xylan derivatives measured by inverse gas chromatography. Colloids Surf A 506:600–606

Velkova N, Doliška A, Zemljič LF et al (2015) Influence of carboxymethylation on the surface physical–chemical properties of glucuronoxylan and arabinoxylan films. Polym Eng Sci 55:2706–2713

Wu Y, Weller CL, Hamouz F et al (2002) Development and application of multicomponent edible coatings and films: a review. Adv Food Nutr Res 44:347–394

Wu Y, Geng F, Chang PR et al (2009) Effect of agar on the microstructure and performance of potato starch film. Carbohydr Polym 76:299–304

Yu-Yue Q, Zhi-Hong Z, Li Lin, Ming-Long Y, Fan Jian, Tian-Rui Z (2015) Physio-mechanical properties of an active chitosan film incorporated with montmorillonite and natural antioxidants extracted from pomegranate rind. J Food Sci Technol 52(3):1471–1479